Nuclear Engineering and Technology 53 (2021) 2816–2829

Contents lists available at ScienceDirect

Nuclear Engineering and Technology

journal homepage: www.elsevier.com/locate/net

Original Article

Uncertainty analyses of spent nuclear fuel decay heat calculations using SCALE modules

Ahmed Shama [a, b, *], Dimitri Rochman [b], Susanne Pudollek [c], Stefano Caruso [d], Andreas Pautz [a, b]

[a] Laboratory of Reactor Physics and Systems Behaviour (LRS), Ecole Polytechnique Fédérale de Lausanne (EPFL), 1015, Lausanne, Switzerland
[b] Laboratory for Reactor Physics and Thermal-Hydraulics (LRT), Paul Scherrer Institute (PSI), 5232, Villigen, PSI, Switzerland
[c] National Cooperative for the Disposal of Radioactive Waste (Nagra), 5430, Wettingen, Switzerland
[d] Kernkraftwerk Gösgen-Däniken AG, 4658, Däniken, Switzerland

ARTICLE INFO

Article history:
Received 20 September 2020
Received in revised form
27 February 2021
Accepted 11 March 2021
Available online 18 March 2021

Keywords:
SNF
SFA
Decay heat
SCALE
Polaris
Sampler
Uncertainty analysis

ABSTRACT

Decay heat residuals of spent nuclear fuel (SNF), i.e., the differences between calculations and measurements, were obtained previously for various spent fuel assemblies (SFA) using the Polaris module of the SCALE code system. In this paper, we compare decay heat residuals to their uncertainties, focusing on four PWRs and four BWRs. Uncertainties in nuclear data and model inputs are propagated stochastically through calculations using the SCALE/Sampler super-sequence. Total uncertainties could not explain the residuals of two SFAs measured at GE-Morris. The combined z-scores for all SFAs measured at the Clab facility could explain the resulting deviations. Nuclear-data-related uncertainties contribute more in the high burnup SFAs. Design and operational uncertainties tend to contribute more to the total uncertainties. Assembly burnup is a relevant variable as it correlates significantly with the SNF decay heat. Additionally, burnup uncertainty is a major contributor to decay heat uncertainty, and assumptions relating to these uncertainties are crucial. Propagation of nuclear data and design and operational uncertainties shows that the analyzed assemblies respond similarly with high correlation. The calculated decay heats are highly correlated in the PWRs and BWRs, whereas lower correlations were observed between decay heats of SFAs that differ in their burnups.
© 2021 Korean Nuclear Society, Published by Elsevier Korea LLC. This is an open access article under the CC BY-NC-ND license (http://creativecommons.org/licenses/by-nc-nd/4.0/).

1. Introduction

The long-term heat generation from accumulated radionuclides within irradiated nuclear fuel, i.e., spent nuclear fuel assemblies (SFAs), impacts the design as well as the operational and long-term safety analyses of radioactive waste management and disposal solutions such as interim storage facilities (ISF) and deep geological repositories (DGR). Prior to commissioning and operation of such facilities, it is necessary to demonstrate their compliance with applicable regulations and to ensure their safety and integrity [2–4]. Impacted activities include loading the SFAs into disposal canisters, for which a maximum heat load per canister is typically constrained. In Switzerland, the maximum permissible limit is 1500 W per canister at emplacement. Such constraints could lead to longer storage times in ISFs prior to encapsulation or the partial filling of disposal canisters, options which are economically disadvantageous. To mitigate these options, optimization studies for canister loading are being conducted that rely on accurate evaluations of the SFA decay heat along with quantification of uncertainties. These inevitable uncertainties in the calculated decay heats place an additional margin on the maximum heat load constraint.

The spent nuclear fuel (SNF) decay heats are typically evaluated by simulating the transmutation and decay of the nuclides in the fuel matrix during the in-reactor irradiation and the out-of-core cooling. The calculational methods are usually validated a priori to assess their performance using validation measures [1,5–7] such as the ratio of the calculated-to-measured decay heat (C/E) and the difference between calculations and measurements ($R = C - E$), or simply the residuals (R). Large deviations between the calculations and measurements mean that more conservative assumptions are

* Corresponding author. Laboratory of Reactor Physics and Systems Behaviour (LRS), Ecole Polytechnique Fédérale de Lausanne (EPFL), 1015, Lausanne, Switzerland.
E-mail address: shama.ahmedsalaheldin@epfl.ch (A. Shama).

https://doi.org/10.1016/j.net.2021.03.013
1738-5733/© 2021 Korean Nuclear Society, Published by Elsevier Korea LLC. This is an open access article under the CC BY-NC-ND license (http://creativecommons.org/licenses/by-nc-nd/4.0/).

needed to account for computational biases and uncertainties in the calculated decay heat. Knowledge of the origin and possible improvement of these discrepancies captured by R and C/E could help to reduce over-conservatism.

Various approaches are followed in the literature to explain the differences between calculations and measurements in calculation-based analyses of SNF. Using similar calculational approaches and different nuclear data evaluations could explain the sources of discrepancies related to the nuclear data. This approach was followed in a study on criticality safety benchmarks by J. C. Sublet that differentiated between JEFF-3.1, ENDF/B-VII and JENDL-3.3 [8]. Other approaches rely on modeling the same benchmark with different codes and code users. The latter approach was followed in various benchmarks conducted by the OECD/NEA on depletion calculations and burnup credit criticality safety [9–11]. Other approaches rely on modeling large numbers of benchmarks using the same calculational methods and nuclear data, so that systematic deviations could be analyzed. The latter approach was followed in various studies conducted in the Oak Ridge National Laboratory on decay heat calculations, depletion calculations, and criticality safety analyses [5,12,13].

In a previous study [1], we followed the latter approach by calculating decay heats for 173 SFAs using the Polaris module of the SCALE code system (version 6.2) [14], and the calculated decay heats were compared to 273 measurements. In the present study, we assess the significance of previously calculated decay heat residuals R by calculating their z-scores, i.e., the ratio of R to its uncertainty. The z-scores scale the differences between calculations and measurements (R) to uncertainties in both, i.e., we test whether SNF decay heat calculations are significantly different from their corresponding measurements or, alternatively, whether the data provide no evidence of such significant differences. We test at a significance level of 0.05. For this goal, we calculate and analyze uncertainties in Polaris decay heat calculations of selected benchmarks from the previous decay heat validation dataset [1]. Four of the selected SFAs are of PWR origin and the other four of BWR origin. They were already used in the decay heat measurements conducted at the Clab facility by SKB [15] (5 SFAs) and the GE-Morris facility by GE [16] (3 SFAs). The assemblies are selected to have multiple decay heat measurements and to differ from each other in their model parameters (burnup, reactor of origin, etc.).

For propagation of uncertainties, stochastic sampling methods are frequently (and recently) used to quantify uncertainties innuclide concentrations, radioactivity, decay heat, and others [17–23]. The method is straightforward once a computational scheme is defined and uncertainties in the inputs are available – such as their covariance matrices. First, computational model inputs – such as nuclear data, design parameters and irradiation histories – are stochastically sampled from their covariance matrices. Second, the perturbed input variables are used in the computational scheme, typically in hundreds of simulation runs, and the distributions of the output responses are analyzed [14]. Calculational uncertainties are propagated from nuclear data (cross-sections, fission yield, and decay data) and model uncertainties using the SCALE/Sampler sequence. Uncertainties in nuclear data (ND) are available in SCALE format, whereas uncertainties in the model parameters (design and operational variables, DO) are based on literature recommendations [24].

Current international projects and benchmarks are addressing questions such as those approached in this study, including the European Horizon 2020 project (European Joint Programme on Radioactive Waste Management [25]), in which calculations of SNF decay heats are compared to experimental measurements and uncertainties in these decay heats are analyzed. Another example is the Vattenfall/SKB-organized blind benchmark on decay heat predictions for 5 PWRs [26], in which decay heats of 5 SFAs and their uncertainties are being calculated and analyzed by several participants using various computational approaches.

This paper is structured as follows. Section 2 provides information about the modeled SFAs. Section 3 describes the calculational methods. Section 4 is divided into three parts: the first part presents the analyses of total calculational uncertainties and z-scores, the second part provides analyses of different contributions from nuclear data and model parameters to the calculational decay heat uncertainties, and the third part provides a discussion on the importance of the burnup uncertainties for the decay heat uncertainties. Section 5 summarizes uncertainty analyses of the SNF decay heat and describes potential future work.

2. SNF benchmarks

A dataset of SNF decay heat benchmarks has been used for validation of the SCALE Polaris module [1], and selected benchmarks are analyzed in the current study to assess uncertainties in their decay heat calculations and their decay heat residuals R. Fig. 1 shows design layouts of the analyzed assemblies based on the design specifications in Refs. [27,28]. Table 1 lists their main characteristics, along with the decay heat residuals from Polaris and reported experimental measurements. The decay heat measurements were conducted by SKB [15] and General Electric (GE) [27,28]. The measurements were conducted at the Clab facility (Swedish Central Interim Storage Facility for Spent Nuclear Fuel) and the GE-Morris facility (Morris Operation spent fuel storage facility), respectively.

The selection criteria for the eight SFAs consist of having different reactors of origin, assembly design, burnup, enrichments, and multiple decay heat measurements. These design and operational differences could result in differences in uncertainties in the calculated decay heats of the analyzed SFAs, propagated from uncertainties in nuclear data and model parameters. The selected assemblies cover wide ranges of burnups, enrichments, and cooling times as shown in Fig. 2. The selected SFAs include 3 from the GE-Morris facility and 5 from the Clab facility. They cover high and low burnups (SFAs F32 and CZ102) as well as high and low enrichments (SFAs D-01 and CZ102) of the validation dataset in Ref. [1]. The shortest cooling time is covered by SFA CZ205, and relatively long cooling times are also covered (e.g., by SFA 5A3).

2.1. Experimental uncertainties in decay heat measurements

The SFA decay heats were measured at both the Clab facility and GE-Morris using pool-type calorimeters. The uncertainties in the calorimetric measurements reported by SKB for the Clab facility are listed in Ref. [15] and are summarized in Table 2. Experimental uncertainties in the measurements conducted at the GE-Morris facility are based on estimates reported by Gauld et al. [5] and are summarized in Table 3. These uncertainties are given as two SDs of the measured decay heat. In the present work, we analyze assemblies with measured decay heat values lying between the upper and lower powers at which uncertainties are reported. Experimental uncertainties at these intermediate decay heat powers are evaluated by linear interpolations between the corresponding values in Tables 2 and 3.

2.2. Input uncertainties for decay heat calculations

Calculated decay heat uncertainties are evaluated through the stochastic propagation of calculational model input uncertainties. These are uncertainties in the SFA design and operational variables (DO) and nuclear data (ND). The latter are uncertainties in the

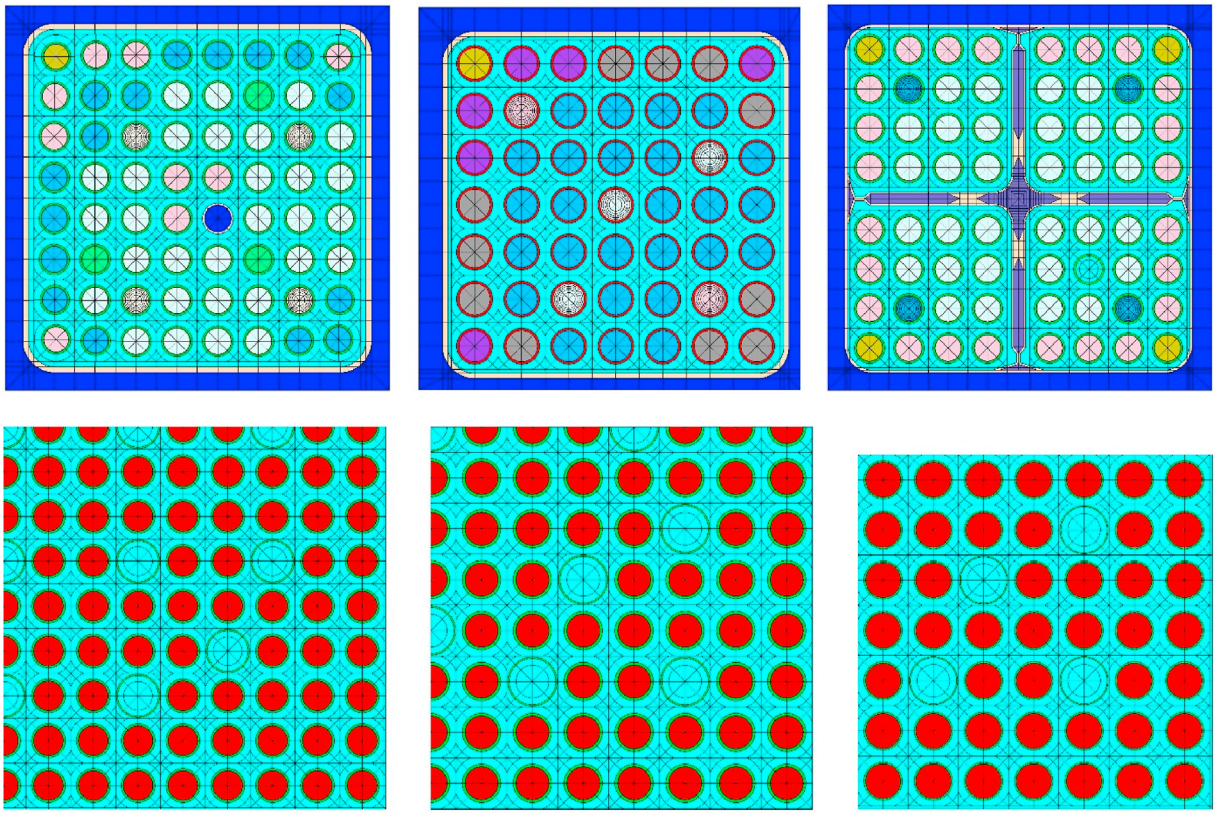

Fig. 1. Polaris models of the analyzed assemblies. Top row: GE 8x8 (6432), GE 7x7 (CZ205 and CZ102), and SVEA-64 (11495). Bottom row: 17x17 (0E2 and 5A3), 15x15 (F32), and 14x14 (D-01). The BWRs are asymmetrical and modeled as full assemblies. The PWRs have quarter symmetry (modeled as south-east models). Within each SFA model, fuel rods are shown in different colors to reflect differences in their density, gadolinium content, and enrichment. (For interpretation of the references to color in this figure legend, the reader is referred to the Web version of this article.)

fission yields (FY), cross-sections (XS), and decay data (DY), which are available in the SCALE code system (version 6.2) based primarily on ENDF/B-VII.1 nuclear data [14]. The DO uncertainties are not available for the currently analyzed benchmarks and they are implemented in this study based on recommended literature values, which are reported in the "Evaluation Guide for the Evaluated Spent Nuclear Fuel Assay Database (SFCOMPO)" [24].

The DO variables are assumed to be normally distributed, and their implemented SDs are listed in Table 4. We assumed that the total mass of the SFA is precise, i.e., the SFA heavy mass has zero variance. This leads to a full correlation between the total cross-sectional area of the fuel rods and the fuel density. Fuel densities are not correlated to irradiation parameters in the current study (e.g., fuel temperatures and burnups). Fuel enrichments of all rods are assumed to be fully correlated. Fuel temperatures, water densities and temperatures, void fractions and the boron content in the water are the same throughout the lattice. In different cycles, these properties are assumed to be fully correlated. No information is available regarding burnup uncertainties in the analyzed SFAs. The cycle-wise powers of the SFAs are assumed to be normally distributed with an SD of 1.67%, which is similar to the value analyzed by Ilas and Liljenfeldt [20]. The SFA cycle-wise average powers are assumed to be fully correlated between cycles. Burnup uncertainties are assumed to originate from uncertainties in the cycle-wise average powers.

Additional correlations were established between water density and temperature in the PWRs, and between SFA power and fuel temperature in both the PWRs and the BWRs. The water temperatures in the PWRs, for example, are sampled from their distribution with a correlation of -1 with the perturbed water density. Similarly, the fuel temperatures are sampled from their distribution with a correlation of $+1$ with the perturbed SFA power. These correlations are based on a large sample of post-irradiation examinations (PIEs) from the SFCOMPO database [29]. However, uncertainties in these correlations are not analyzed in this study.

The Polaris models are 2D lattice models that represent full-length SFAs. In addition, we followed simplified irradiation histories, e.g., cycle-wise average irradiation parameters. Given these modeling simplifications, the uncertainties mentioned in Table 4 should be interpreted as uncertainties in the average DO variables of the SFAs and uncertainties in the cycle-wise average irradiation parameters. Given that DO variables and irradiation parameters could vary significantly along the entire SFA geometry and during fine representations of irradiation histories, we implement uncertainties in their assembly or cycle-wise averages. For example, the void fraction in BWRs changes axially, and the implemented values are uncertainties in the axially averaged void fractions. Similarly, uncertainties in the boron content, which change during the irradiation cycle, represent uncertainties in the cycle-wise average values.

Burnup will prove to be a significant variable that impacts the resulting uncertainties of DO origin, and the accuracy of the burnup estimation depends on various factors, such as the reactor and core management codes [24]. It also typically depends on the location in the core, i.e., whether it is located in the periphery of the core or its center. For this reason, we will analyze cases in addition to those listed in Table 4, focusing only on the SFA 6432. For these cases, the burnup and power assumptions are relaxed and assessed for their relevance to the resulting uncertainties, and we compare them to the reference case mentioned in Table 4. The following cases are

Table 1
Characteristics of the analyzed SFAs and their decay heat measurements.

Lab.	Reactor [a]	SFA ID	SFA design[+]	Enrichment	Burnup	Cooling time	Decay heat [b]	$2\sigma_{exp.}$ [b]		R [1] [c]
				wt.% U-235	GWd/tU	a	W	W/SFA	W/tU	W
Clab (SKB)	F2 (BWR)	11495	SVEA-64	2.91	32.43	15.32	167.6	5.0	27.5	−0.9
	R1 (BWR)	6432	AA8x8 (GE 8x8)	2.89	36.86	14.85	185.5	5.1	28.7	2.3
						14.86	189.6	5.1	28.9	−1.7
						15.53	184.4	5.1	28.7	0.7
						15.56	182.8	5.1	28.6	2.2
						15.56	185.2	5.1	28.7	−0.2
						15.58	181.6	5.1	28.6	3.3
						15.58	182.0	5.1	28.6	3.0
						17.60	175.9	5.0	28.4	1.5
						20.61	161.7	4.9	27.9	5.7
						20.62	161.7	4.9	27.9	5.6
GE-Morris (GE)	C (BWR)	CZ102	GE 7x7	1.09	11.67	6.94	62.3	12.7	64.9	18.8
						7.16	70.4	12.9	65.9	9.6
		CZ205	GE 7x7	2.50	25.34	2.35	324.0	19.0	99.8	1.2
						2.38	361.5	19.9	104.5	−39.7
						2.39	343.5	19.4	102.2	−22.6
						2.39	353.2	19.7	103.5	−32.5
						2.43	331.8	19.2	100.8	−15.3
						2.43	338.7	19.3	101.6	−22.4
						2.44	327.5	19.1	100.2	−12.7
						2.45	313.1	18.7	98.4	0.5
						2.46	311.4	18.7	98.2	1.5
						2.47	314.0	18.7	98.5	−1.5
						2.56	331.2	19.1	100.7	−28.2
						2.59	317.1	18.8	98.9	−16.8
						2.98	289.7	18.2	95.4	−20.4
						3.02	308.0	18.6	97.7	−41.3
GE-Morris	SO1 (PWR)	D-01	14x14	4.01	31.39	6.46	499.0	23.2	63.7	−8.4
Clab	R2 (PWR)	F32	15x15	3.20	50.96	16.05	692.0	15.7	36.0	9.8
	R3 (PWR)	0E2	W 17x17	3.10	41.63	15.95	587.9	14.2	30.6	3.2
						17.50	566.0	13.9	29.9	6.1
						17.51	567.7	13.9	30.0	4.4
						21.44	522.5	13.2	28.5	7.4
						21.47	525.6	13.3	28.6	4.3
						21.84	520.1	13.2	28.4	6.1
		5A3	W 17x17	2.10	19.70	19.10	237.7	9.0	19.5	0.1
						19.11	236.7	9.0	19.5	1.1
						19.12	243.4	9.1	19.7	−5.6
						19.98	230.9	8.9	19.3	3.4
						20.01	230.3	8.9	19.3	3.9
						21.05	225.8	8.8	19.2	4.3
						21.07	227.9	8.9	19.2	2.2
						25.94	209.8	8.6	18.6	2.8

[a] Reactor names: F = Forsmark, R = Ringhals, C = Cooper, and SO = San Onofre.
[b] Measured decay heats and their uncertainties (per assembly and per ton of initial uranium) [15,27,28].
[c] Calculated decay heat residuals *R* between Polaris calculations and measurements [1].

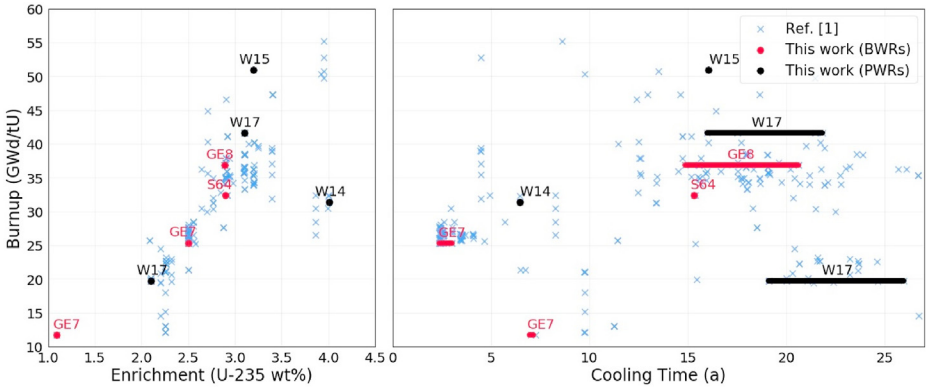

Fig. 2. Burnups, enrichments, and cooling times of the selected SFAs. The crosses refer to the entire validation dataset in Ref. [1].

Table 2
Uncertainties (2σ) in the decay heat measurements at the Clab facility based on [15].

SFA	Power (W)	Uncertainty (W)	Uncertainty (%)
BWR	50	4.2	8.4
	350	6.2	1.8
PWR	250	9.2	3.7
	900	18.8	2.1

Table 3
Uncertainties (2σ) in the decay heat measurements at the GE-Morris facility based on [5]. The values correspond to both PWRs and BWRs.

SFA	Power (W)	Uncertainty (W)	Uncertainty (%)
GE	200	16	8
	700	28	4

analyzed for the SFA 6432:

1 Case 1: The upper and lower accuracies of the burnup in Ref. [24] are interpreted as 2 SD, and therefore the SD of the burnup increases by 50% including every other variable. For example, cycle-wise powers are normally distributed with an SD of 2.5% instead of 1.67%.
2 Case 2: All variables are uniformly distributed. The variance of each distribution for each variable is set equal to the variance of the corresponding normal distribution of the variable in the reference case. For example, burnup is uniformly distributed between 0.971 and 1.029 of its nominal value, instead of normal distribution with an SD of 1.67%.
3 Case 3: Burnup uncertainty is considered (both cycle-wise average powers and the correlated fuel temperatures), and nominal values are used for all other variables to exclude their influence on the resulting decay heat uncertainty.
4 Cases 4 and 5: The uncertainty in the cycle-wise powers depends on the burnup, i.e., instead of a fixed SD of 1.67% of the cycle-wise powers in the nominal case, the variance of the cycle-wise power depends on the current burnup value. Assemblies are relocated to different regions of the core in different irradiation cycles and, as noted in Ref. [24], uncertainties in powers and burnups could be larger in peripheral locations of the core. In-out, out-in, and in-out-in (along with others [30]) are fuel-loading strategies that allocate the assemblies in the core based on their reactivities and burnup; this could result in assemblies having uncertainties in their powers depending on their current location in the core and their current burnup value.

We consider two relatively extreme cases: the first case has zero variance in the SFA power at BOL (beginning of life), and the variance in the cycle-wise powers increases linearly with burnup up to discharge. The second case has a maximum variance in the SFA power at BOL, and the variance in the cycle-wise powers decreases linearly with burnup up to zero variance at discharge. In both cases, the SFA discharge burnup has the same SD of 1.67%. For example, for the first case of zero variance in the power at BOL, the SD of the cycle-wise powers are 0.2% and 3.2% for the first and the last irradiation cycles, respectively.

5 Case 6: The cycle-wise powers are sampled from their distributions independently from each other, i.e., correlations are not enforced. The discharge burnup does not necessarily have the nominal SD.

Finally, uncertainties in other design parameters are not covered in Ref. [24] and can scarcely be found in the literature. These include uncertainties in the gap between assemblies and the location of fuel rods in relation to each other. An individual case of SFA 6432 has been analyzed to investigate the contributions of these parameters to total calculational uncertainties by allowing them to follow normal distributions bounded by ±3 SD (between 0.1 and 14.2 mm for the former, and between 0.25 and 1.75 mm for the latter). The decay heat variances due to perturbations in DO parameters changed by less than 0.7% up to a cooling period of 100 years. Given their relatively modest contributions to calculational uncertainties, we excluded these variables from the analysis in this study.

3. Computational scheme

The decay heat calculations in the current study are performed using version 6.2 of the SCALE nuclear modeling and simulation code system [14]. The SCALE code system is widely used for nuclear system design and safety analyses such as criticality safety, shielding calculations, LWR analyses, etc. Two SCALE modules were used here: the Polaris module and the Sampler super-sequence. The Polaris module performs the lattice calculations (transport, depletion and decay). A result of the Polaris calculations is the cooling time-dependent decay heat per nuclide of the analyzed SFAs. The assumptions for the implementation of the models in Polaris were described previously [1]. All calculations are based on the SCALE 56-group library. The decay and fission yield data are based on the ENDF/B-VII.1 nuclear data library. The multigroup (MG) neutron cross-section libraries are based primarily on ENDF/

Table 4
Uncertainties in DO variables of the analyzed SFAs, based on [24].

Parameter [a]	Uncertainty/Tolerance [24]	1 σ (this work)
Cladding/tube thickness	±40–50 μm	16.7 μm [c]
Cladding/tube diameter	±200 μm (PWR)/± 300 μm (BWR)	67 μm/100 μm [c]
Fuel pellet density	<2% the theoretical density	0.67% [c]
Fuel pellet diameter	±20 μm	[b]
Enrichment (U-235 wt%)	±0.05%	0.0167% [c]
SFA powers	–	1.67%
Water temp. (PWR only)	±2 °C	2 °C
Water density (PWR only)	±0.005 g/cm^3	0.005 g/cm^3
Void fraction (BWR only)	±6%	6%
Fuel temp.	±50 °C	50 °C
Boron content (PWR only)	±10 ppm	10 ppm

[a] The parameters in Ref. [24] not included in this list are assumed to be precise.
[b] Full correlation with fuel density.
[c] The reported uncertainties in Ref. [24] are tolerances, and we assume that a two-sided tolerance interval contains ~99.7% of the observations, i.e., the tolerance interval corresponds to ±3 σ of a normal distribution.

B-VII.1 along with supplementary data from the JEFF-3.0/A nuclear data library, which is recommended for general-purpose reactor physics and LWR analysis [14].

The Sampler super-sequence performs stochastic uncertainty propagations [22]. Sampler generates and runs hundreds of input files of sub-sequences (Polaris) and analyzes the outputs. The inputs are generated by random sampling from nuclear data covariances (available in SCALE) and joint probability distributions of uncertain DO variables (listed in Table 4). The outputs are statistical analyses of distributions of Polaris calculations of the decay heat per nuclide and per SFA.

4. Results

Decay heats and their uncertainties for each of the analyzed SFAs are calculated from a set of decay-heat-relevant nuclides, i.e., the total decay heat of each SFA is the sum of decay heats of the individual decay-heat-relevant nuclides. We considered nuclides that contribute $\gtrsim$ 99% to both decay heat and decay heat uncertainty as evaluated according to Equations (1) and (2), respectively, and at cooling times between 2 and 100 years. The nuclide-wise contribution to decay heat relates to the nuclide-wise radioactive decay rate and the Q-value of each radionuclide considered. The nuclides are Kr-85, Sr-90, Y-90, Rh-106, Sb-125, Pr-144, Cs-134, Cs-137, Ba-137 m, Ce-144, Pm-147, Eu-154, Pu-238, Pu-239, Pu-240, Pu-241, Am-241, Am-243, Cm-242, and Cm-244. In the following equations, we use i and j (subscripts and superscripts) for different isotopes, DH for decay heat, k for different perturbations, N for total number of perturbations, and n and m (subscripts and superscripts) for different benchmarks (measurements and calculations). The total decay heats and their uncertainties are calculated such that:

$$DH_{total} = \sum_i DH_i, \tag{1}$$

$$\sigma^2_{total} = \sum_i \sigma_i^2 + \sum_{i,j} 2\sigma_i\sigma_j\rho_{ij}, \tag{2}$$

where $\rho_{i,j}$ refers to the correlation between each pair of nuclides i and j in the list of nuclides considered. In Equation (2), σ_i^2 and σ_i are the variance and the SD of the decay heat of nuclide i, respectively. These statistics result from numerous runs of the models using perturbed inputs, and are calculated using:

$$\sigma_i = \sqrt{\frac{1}{N-1}\sum_k^N \left(DH_k - \overline{DH}_i\right)^2}, \tag{3}$$

where $\overline{DH}_i$is the average decay heat from isotope i.

The correlations in Equation (2) result from using the same perturbed ND in numerous runs. These correlations exist between decay heats of a nuclide in two SFAs and also between the decay heats of different nuclides in the same SFA. The correlation between the decay heat of nuclides i and j is calculated as:

$$\rho_{ij} = \frac{1}{N-1}\sum_{k=1}^N \frac{\left(DH^i{}_k - \overline{DH}_i\right)\left(DH^j{}_k - \overline{DH}_j\right)}{\sigma_i\,\sigma_j}, \tag{4}$$

Polaris models are run 625 times using various perturbed inputs, e.g., perturbed FY, XS, DO variables, etc. The number of 625 perturbed runs is selected to ensure that the results are sufficiently precise, i.e., they have low standard errors (SE). The SEs of SDs and correlation coefficients are calculated as [31]:

$$SE(\sigma_i) = \frac{\sigma_i}{\sqrt{2\times 625}},\ SE(\rho_{ij}) = \frac{1-{\rho_{ij}}^2}{\sqrt{625-1}}. \tag{5}$$

The mean calculated decay heats are not reported in the current analyses. Instead, we report those decay heats calculated using the nominal ND files (Equation (1)). In all of the analyzed models, the differences between the mean calculated decay heats and the decay heats resulting from the use of the nominal ND are less than the SEs of the former statistic. The SEs of SDs and correlation coefficients depend on their values, e.g., in Section 4.3 assembly F32 shows 2σ of 49.0 W for its total decay heat due to uncertainties in ND. The latter uncertainty will have an SE of 1.4 W, which is 2.8%. In Section 4.6, the total decay heat of the same assembly shows correlations of 0.67 and 0.98 with the total decay heats of assemblies 5A3 and 0E2, respectively. The latter correlations will have SEs of 2.2% and 0.2%, respectively.

The uncertainties in the DO variables and their correlations are discussed in Section 2.2. The ND uncertainties concern FY, XS and DY, and the latter are assumed to be uncorrelated with each other. The decay heat uncertainty for nuclide i resulting from ND uncertainties is calculated as:

$$\sigma^2_{ND,\,i} \cong \sigma^2_{XS,i} + \sigma^2_{FY,i} + \sigma^2_{DY,i}. \tag{6}$$

The ND are assumed to be uncorrelated with DO variables, and the total decay heat uncertainty for nuclide i resulting from calculational uncertainties is calculated as:

$$\sigma^2_{Calc.,i} \cong \sigma^2_{ND,i} + \sigma^2_{DO,i}, \tag{7}$$

The total calculated and experimentally measured decay heats are assumed to be uncorrelated with each other. Uncertainty of the decay heat residuals R of benchmark i is calculated from calculational and measurement uncertainties as:

$$\sigma^2_{R,i} = \sigma^2_{Calc.,Exp.,i} \cong \sigma^2_{Calc.,i} + \sigma^2_{Exp.,i}, \tag{8}$$

4.1. Total decay heat generation: calculations and measurements

Decay heats and their uncertainties have been calculated for the SFAs listed in Table 1, and the results are shown in Fig. 3. This figure shows the decay heats of the SFAs (in W/tU) versus the cooling time along with decay heats from the fission and decay products (F/DP) and actinides (AC). Fission and decay products refer to nuclides with atomic number $Z \leq 89$. Uncertainty bands of the calculations ($2\sigma_C$) are shown along with error bars of the experimental measurements ($2\sigma_E$).

The F/DPs dominate the decay heat generation up to 50–70 years of cooling, and the longer-lived ACs become the main sources of the decay heat thereafter. In the short term, decay heat uncertainties mainly result from uncertainties in the F/DPs. Additionally, for the high burnup SFAs 0E2 and 6432, uncertainties from the ACs dominate earlier – e.g., at 9–10 years of cooling. Fig. 3 is arranged such that the top row contains the higher burnup SFAs, and the left half (two left columns) contains the SFAs of PWR origin. The high burnup SFAs produce higher decay heats per ton of uranium, particularly at shorter cooling times, due to their higher content of decay-heat-generating ACs and F/DPs. Additionally, their calculational uncertainties (total and in F/DPs and ACs) are higher than the low burnup SFAs.

No significant differences are noted between PWRs and BWRs (in terms of their decay heats and the corresponding uncertainties), and the SFA burnup is seen to produce significant differences in

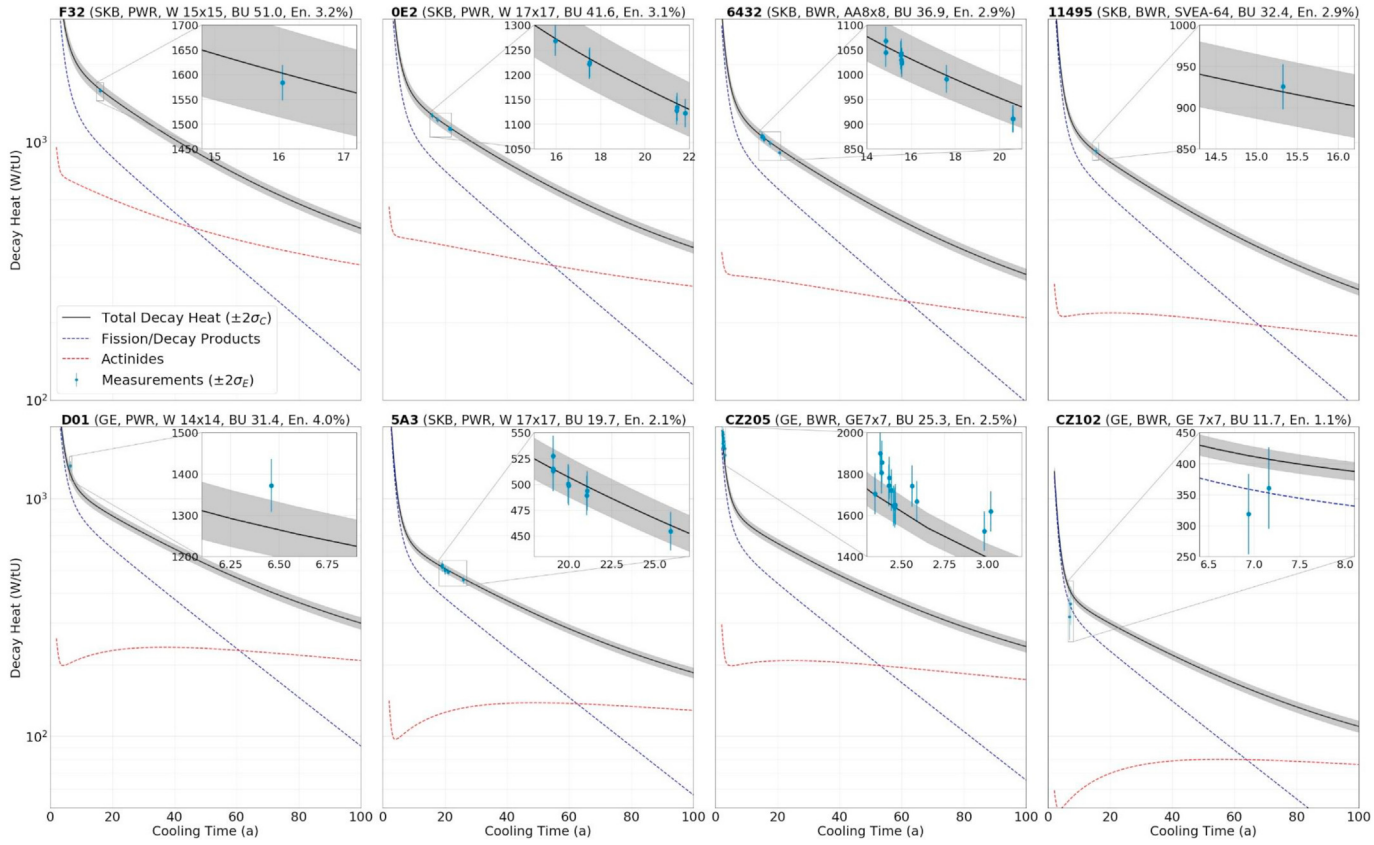

Fig. 3. Calculated total decay heats and uncertainties (due to ND and DO variables). Uncertainty bands are $2\sigma_C$. Error bars are $2\sigma_E$. The top row shows high-burnup SFAs. The two left columns are PWRs. The top legends correspond to: SKB and GE, reactor of origin, burnup (GWd/tU), and U-235 enrichment (wt.%).

decay heat uncertainties. Differences are noted between the Clab and GE-Morris SFAs, as experimental uncertainties in the latter are relatively higher. All calculated decay heats of the Clab SFAs intersect with the smaller $2\sigma_E$ bars, which is not the case for the GE-Morris SFAs, which have larger $2\sigma_E$ bars.

4.2. Hypothesis testing using z-scores of the decay heat residuals

In this study, we test the null hypothesis that the calculated decay heat (C) and the measured value (E) are equal:

$$H_0 : C - E = 0. \tag{9}$$

The alternative hypothesis is that they are significantly different: $H_a : C \neq E$.

The decay heat calculations and measurements are converted into z-scores [31,32]. The means and the variances are known for the calculations and the measurements, and their total uncertainties ($2\sigma_{C,E}$) scale their differences. The z-score of benchmark m is calculated as:

$$z_m = \frac{C_m - E_m}{\sigma^m_{C,E}}. \tag{10}$$

The z-scores are used to obtain p-values and, for the SFAs analyzed in this work, a value of $z = 1.96$gives a threshold p-value $\cong 0.05$. A value of $|z| < 1.96$ indicates that the difference between the calculated and the measured decay heat could be explained by their total uncertainty.

For SFAs that have multiple measurements, and therefore calculations, their z-scores are combined into a single figure using a combined weighted z-transform [33,34]. We use the following transformation to obtain the SFA combined z-score:

$$\overline{z} = \frac{\sum_{m=1}^{M} w_m z_m}{\sqrt{\sum_{m=1}^{M} {w_m}^2 + 2\sum_{m<n}^{M} w_m w_n \rho_{mn}}} \tag{11}$$

where w_m is a weight for z_m, and ρ_{mn} is the correlation between z_m and z_n. The benchmarks of SFAs with multiple measurements were assigned equal weights in this study. Correlations between the z-scores were obtained from the covariances between the calculations and the standard deviations of the combined measurements and calculations as following:

$$\rho_{mn} = \frac{cov(R_m, R_n)}{\sigma^m_R \sigma^n_R} \cong \frac{cov(C_m, C_n)}{\sigma^m_R \sigma^n_R}. \tag{12}$$

The above approximation of the covariances between the residuals into covariances between the calculations results from assuming that different measurements (measurements m and n) have zero covariances, and measurements and calculations also have zero cross-covariances. Indeed, no covariance is reported for the decay heat measurements, and therefore only the covariances between calculations contribute to covariances between the residuals. Such approximations used in Equation (12) result in lower correlations between different tests on the same SFA, and therefore a higher combined z-score for the entire SFA benchmarks. The combined test for an SFA is conservative, i.e., it is more likely to reject the null hypothesis and conclude that calculations and measurements differ significantly from each other. Access to

covariance information between measurements could reduce this conservatism to give more accurate p-values. The combined z-scores are shown in Fig. 4 for each SFA. The figure also plots the residual R versus the mean of the calculations and the measurements for each benchmark, along with uncertainty bands of $2\sigma_{C,E}$.

For the Clab SFAs and the GE-Morris PWR SFA, the SFA combined z-scores are within the threshold value of 1.96, which implies agreement between the calculations and the measurements, i.e., the combined uncertainty of the decay heat calculations and the measurements $\sigma_{C,E}$ could explain the observed differences between both, and we fail to reject the null hypothesis. In contrast, for the GE-Morris BWR SFAs, and given the combined z-scores, we reject the null hypothesis in favor of the alternative, i.e., the differences between the calculations and the measurements are significant and could not be explained by relatively wide bands of total uncertainties. A comparison based solely on the z-score could be misleading due to a high variance in either the calculations or the measurements, i.e., large uncertainties in either C or E could result in an overlap of the differences between them. The uncertainties of C and E are examined individually as shown in Table 5, which lists these uncertainties in each of the analyzed SFAs. The measurements at Clab are some of the least uncertain in the literature, with approximately 19–36 W for $2\sigma_E$, which also contributes to lower combined uncertainties of the measurements and the calculations. Nevertheless, the residuals between the present calculations and the corresponding measurements were contained within the relatively narrow bands of $2\sigma_{C,E}$ The measurements at GE-Morris have large experimental uncertainties ($2\sigma_E$ are 64–100 W/tU) but they do not explain the relatively large residuals of 73 W/tU, and −94 W/tU observed in SFAs CZ102 and CZ205, respectively. Nevertheless, these residuals are similar to other literature values [5], which rely on different calculational methods. The relatively larger total uncertainties could not explain these residuals of the SFAs CZ102 and CZ205. This suggests that either their DO data or measurements fail to account for some additional random or systematic error components of uncertainties. It also highlights the importance of decay heat measurements that properly address possible sources of measurement uncertainties or systematic deviations, in addition to the availability of accurate operational and design information.

4.3. Contribution of ND and DO uncertainties

Calculations, measurements, and total decay heat uncertainties change relatively smoothly during the analyzed cooling times. For instance, between the shortest and longest cooling times of 14.9 and 20.6 years for SFA 6432, the measurement uncertainties (2 SD) change between 2.7% and 3.1%. Also, the calculational uncertainties change between 4.4% and 4.5%, which adds to combined total uncertainties that change between 5.3% and 5.4%. For this reason, we analyze total decay heat uncertainties averaged over the analyzed cooling times.

Assembly-wise averages of the calculational uncertainties ($2\sigma_C$) are listed in Table 5. These uncertainties originate from uncertainties in ND and DO variables, and their implementation in this study is discussed in Section 2.2. Table 6 lists individual contributions from ND and DO variables to the total calculational uncertainties. Decay heat uncertainties of DO origin contribute more to the total calculational uncertainties of all analyzed SFAs, particularly lower burnup SFAs, than uncertainties of ND origin. The latter tend to apply more to high burnup SFAs. In the PWR SFAs, the uncertainties of ND origin are 1.1–3.1% of the total decay heat (the average of the calculated and the measured values), and 1.1–1.8% in the BWR SFAs.

4.4. Nuclides relevant for decay heat uncertainties

The calculational uncertainties discussed so far originate from nuclides that contribute more than 99% to decay heats and decay heat uncertainties at cooling times between 2 and 100 years. The analyses hereafter focus on nuclides that are relevant to decay heats and decay heat uncertainties at the average cooling times of the analyzed SFAs – the average cooling time of the decay heat measurements of each SFA. The nuclides considered contribute more than 97% and 97.5% to the calculated decay heats and decay heat uncertainties in the analyzed SFAs, respectively. The nuclides are Sr-90, Y-90, Rh-106, Pr-144, Cs-134, Cs-137, Ba-137 m, Eu-154, Pu-238, Pu-239, Pu-240, Am-241, Cm-242, and Cm-244. Their contributions to the total calculational uncertainties and the calculational uncertainties of ND origin are listed in Table 7 at selected cooling times for each SFA. We present the contribution per nuclide as 2σ (W/tU). Cm-242 is excluded from the table due to

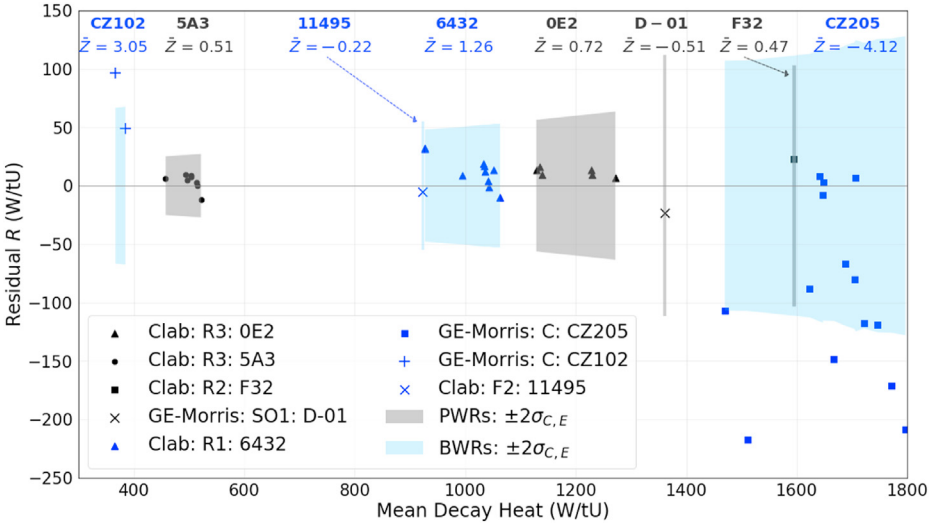

Fig. 4. Mean-difference plot of calculations and measurements along with shaded total uncertainty band $2\sigma_{C,E}$. Combined z-scores are shown for each SFA (top). The legend lists the measurement laboratories, reactors of origin, and SFA IDs.

Table 5
Average uncertainties of the analyzed SFAs.

Reactor of origin	SFA ID	Burnup (GWd/tU)	Avg. cooling [a] time (a)	Avg. decay heat [b] (W/tU)	Meas. ($2\sigma_E$)		Calc. ($2\sigma_C$)		Total ($2\sigma_{C,E}$)	
					W/tU	%	W/tU	%	W/tU	%
PWRs	F32	51.0	16.1	1595	36	2.3	90	5.6	97	6.1
	OE2	41.6	19.3	1188	29	2.5	58	4.9	65	5.5
	D-01	31.4	6.5	1361	64	4.7	66	4.9	92	6.8
	5A3	19.7	20.7	501	19	3.9	19	3.8	27	5.4
BWRs	6432	36.9	16.6	1015	29	2.8	47	4.6	55	5.4
	11495	32.4	15.3	923	28	3.0	39	4.2	47	5.1
	CZ205	25.3	2.5	1667	100	6.0	67	4.0	121	7.2
	CZ102	11.7	7.1	376	65	17.4	15	4.1	67	17.9

[a] Average cooling times of the SFAs.
[b] Average calculated and measured decay heats of the SFAs.

Table 6
Contributions of ND and DO variables to calculational uncertainties.

Reactors of origin	SFA ID	Burnup (GWd/tU)	Avg. cooling [a] time (a)	Calc. uncertainties ($2\sigma_C$)					
				ND		DO		Total	
				W/tU	%[b]	W/tU	%[b]	W/tU	%[b]
PWRs	F32	51.0	16.1	49	3.1	75	4.7	90	5.6
	OE2	41.6	19.3	26	2.2	51	4.3	58	4.9
	D-01	31.4	6.5	19	1.4	63	4.7	66	4.9
	5A3	19.7	20.7	5	1.1	18	3.6	19	3.8
BWRs	6432	36.9	16.6	18	1.8	43	4.2	47	4.6
	11495	32.4	15.3	13	1.4	36	3.9	39	4.2
	CZ205	25.3	2.5	25	1.5	63	3.8	67	4.0
	CZ102	11.7	7.1	4	1.1	15	4.0	15	4.1

[a] Average cooling times of the SFAs.
[b] Ratio of $2\sigma_C$ to the total decay heat (average calculated and measured values).

Table 7
Contributions, by nuclide, to decay heat uncertainties (2σ)due to uncertainties in ND, and uncertainties in ND and DO variables combined.

Reactor of origin	SFA ID	Burnup (GWd/tU)	Cooling (a)	Uncertainty origin	Sr-90	Y-90	Rh-106	Cs-134	Cs-137	Ba-137 m	Pr-144	Eu-154	Pu-238	Pu-239	Pu-240	Am-241	Cm-244	Total (W/tU)
PWR	F32	51.0	16.1	ND	1.1	5.8	0.0	0.9	0.8	1.5	0.0	4.4	19.6	0.4	0.9	4.8	43.7	49
				Total	2.0	9.6	0.0	1.0	3.7	12.7	0.0	4.6	24.4	0.6	1.0	6.5	53.7	90
	0E2	41.6	21.8	ND	0.9	4.6	0.0	0.1	0.6	1.2	0.0	2.3	12.2	0.4	0.7	4.8	19.5	25
				Total	1.6	7.9	0.0	0.1	2.8	9.6	0.0	2.4	15.5	0.6	0.9	7.5	23.9	54
	D-01	31.4	6.5	ND	1.1	5.7	1.1	12.5	0.7	1.3	0.1	4.6	8.1	0.4	0.5	1.6	7.8	19
				Total	2.2	10.6	2.4	15.0	3.0	10.3	0.5	5.2	11.5	0.8	0.7	3.4	9.9	66
	5A3	19.7	25.9	ND	0.4	2.2	0.0	0.0	0.3	0.5	0.0	0.5	3.0	0.3	0.4	2.4	1.5	5
				Total	0.8	3.9	0.0	0.0	1.2	4.2	0.0	0.5	3.8	0.4	0.5	4.6	1.9	18
BWR	6432	36.9	17.6	ND	0.9	4.5	0.0	0.3	0.6	1.1	0.0	2.3	9.6	0.3	0.7	3.3	13.7	18
				Total	1.6	7.8	0.0	0.3	2.6	9.0	0.0	2.4	12.8	0.6	0.9	5.6	17.5	45
	11495	32.4	15.3	ND	0.9	4.5	0.0	0.6	0.6	1.1	0.0	2.3	7.3	0.3	0.6	2.5	9.1	13
				Total	1.6	8.0	0.0	0.8	2.5	8.7	0.0	2.5	9.8	0.5	0.8	4.3	11.8	39
	CZ205	25.3	3.0	ND	0.8	4.0	1.4	8.4	0.5	1.0	0.2	3.4	7.8	0.3	0.5	1.5	9.2	23
				Total	1.5	7.4	2.9	10.3	2.4	8.1	0.7	3.8	10.6	0.6	0.7	2.5	11.5	67
	CZ102	11.7	7.2	ND	0.4	2.1	0.3	2.0	0.2	0.5	0.0	0.8	2.4	0.2	0.2	0.7	0.5	4
				Total	0.8	4.1	0.5	2.3	1.1	3.8	0.1	0.9	2.8	0.4	0.3	1.5	0.6	15

its very low contribution to decay heat uncertainties, except at very short cooling times such as for SFA CZ205. Due to uncertainty in both ND and DO variables, the 2σ of this SFA drops from 6.3 to 0.2 W/tU between the cooling times of 2.3 and 3.0 years.

The SFAs measured at shorter cooling times (2–7 years), such as CZ102, CZ205 and D-01, show larger contributions from Rh-106, Pr-144, Cs-134 and Cm-242 compared to the other SFAs. The short-lived Rh-106 is in transient equilibrium with its parent Ru-106, which has a half-life of 1.02 years [35]. At short cooling times, they show contributions to decay heat uncertainties; however, at cooling times $\gtrsim$ 15 years, their contributions are nearly zero. Similarly, the short-lived Pr-144 and Pr-144 m are in transient equilibrium with the parent Ce-144, which has a half-life of 285 days. Cs-134 has a half-life of 2.07 years and is mainly produced during irradiation from neutron capture by Cs-133. The contributions from Cs-134 are lower at longer cooling times; however, its half-life is not as short as the former nuclides. Cm-242 also accumulates during irradiation; however, its short half-life of 163 days reduces its total decay heat significantly in SFAs measured at longer cooling times. The remaining Cm-242 approaches secular equilibrium with its parents Am-242 and Am-242 m. Cm-244 is a major nuclide that contributes to both decay heat and decay heat uncertainties and accumulates with burnup. In the PWR SFAs, uncertainties resulting from Cm-244 show monotonic increases with burnup up to 45% in the highest burnup SFA F32, due to uncertainties in both ND and DO variables. In this SFA, and at the average time of measurements, Cm-244 contribution to the decay heat uncertainties is considerably higher than its contribution to

the decay heat, which is 15%. Pu-238 shows similarity to Cm-244, as it is also a major nuclide that contributes to both decay heat and decay heat uncertainties and accumulates with burnup. It also shows that its contributions to decay heat uncertainties are significantly higher than its contributions to decay heats, particularly in lower burnup SFAs. For example, in the lowest burnup PWR SFA (5A3), Pu-238 contributes 6.2% to the decay heat and 17% to the decay heat uncertainties (due to uncertainties in ND and DO variables).

4.5. Contributions of XS, FY, DY and ND uncertainties

The contributions of uncertainties in XS, FY, and DY to uncertainties of ND origin, and the contributions of ND uncertainties to calculational uncertainties, will be presented as fractional variances (FVs). The XS contributions to uncertainties of ND origin are calculated as:

$$FV_{XS} = \frac{\sigma_{XS}^2}{\sigma_{ND}^2} = \frac{\sigma_{XS}^2}{\sigma_{XS}^2 + \sigma_{FY}^2 + \sigma_{DY}^2}. \quad (13)$$

The ND contributions to calculational uncertainties of ND and DO origin are calculated as:

$$FV_{ND} = \frac{\sigma_{ND}^2}{\sigma_{Total}^2} = \frac{\sigma_{ND}^2}{\sigma_{ND}^2 + \sigma_{DO}^2}. \quad (14)$$

Fractional variances due to XS, FY and DY uncertainties and also due to ND uncertainties are shown in Fig. 5 for decay-heat-relevant nuclides, and for six of the analyzed SFAs with higher burnups. The figure shows these values between 2 and 48 years of cooling after discharge. For instance, for Sr-90 in the SFA CZ205 (bottom left plot in Fig. 5), the FV due to ND is ~0.25 (gray area) and the FV due to DO is ~0.75 (the remaining white area). Similarly, in the same plot, the FVs due to XS, FY and DY are approximately 0.07, 0.70, and 0.23, respectively.

Contributions from ND to the total variances are almost constant along the investigated decay times (2–48 years) for the majority of the analyzed nuclides. Actinides such as Pu-240, Am-241 and Cm-242 show changes in the contributions of ND to the total variances. The concentrations of the latter ACs change significantly during the analyzed cooling times, as they are being produced from decay processes of other actinides. Pu-240 (with a half-life of 6.6×10^3 years) is actively produced through alpha decay of Cm-244 (with a half-life of 18.1 years). Am-241 (with a half-life of 433 years) is actively produced through beta decay of Pu-241 (with a half-life of 14.3 years). Cm-242 (with a half-life of 163 days) approaches secular equilibrium with its parents Am-242 and Am-242 m (with half-lives of 16 h and 141 years, respectively).

Differences between the production routes of decay-heat-relevant nuclides result in different contributions of XS, FY and DY data to uncertainties of ND origin. For the ACs, ND variances are largely due to XS (0.97–0.99) and, to a minor extent, to DY (0.01–0.03). The F/DPs show different contributions from XS, FY and DY. Fission yield uncertainties contribute significantly to uncertainties of ND origin for both Sr-90 and Y-90. Uncertainties in DY also contribute to both, whereas DY contributions to the daughter (Y-90) are higher. Ba-137 m and Cs-137 also exist in secular equilibrium, and their uncertainties of ND origin are also significantly due to uncertainties in FY and DY. The short-lived Pr-144 and Rh-

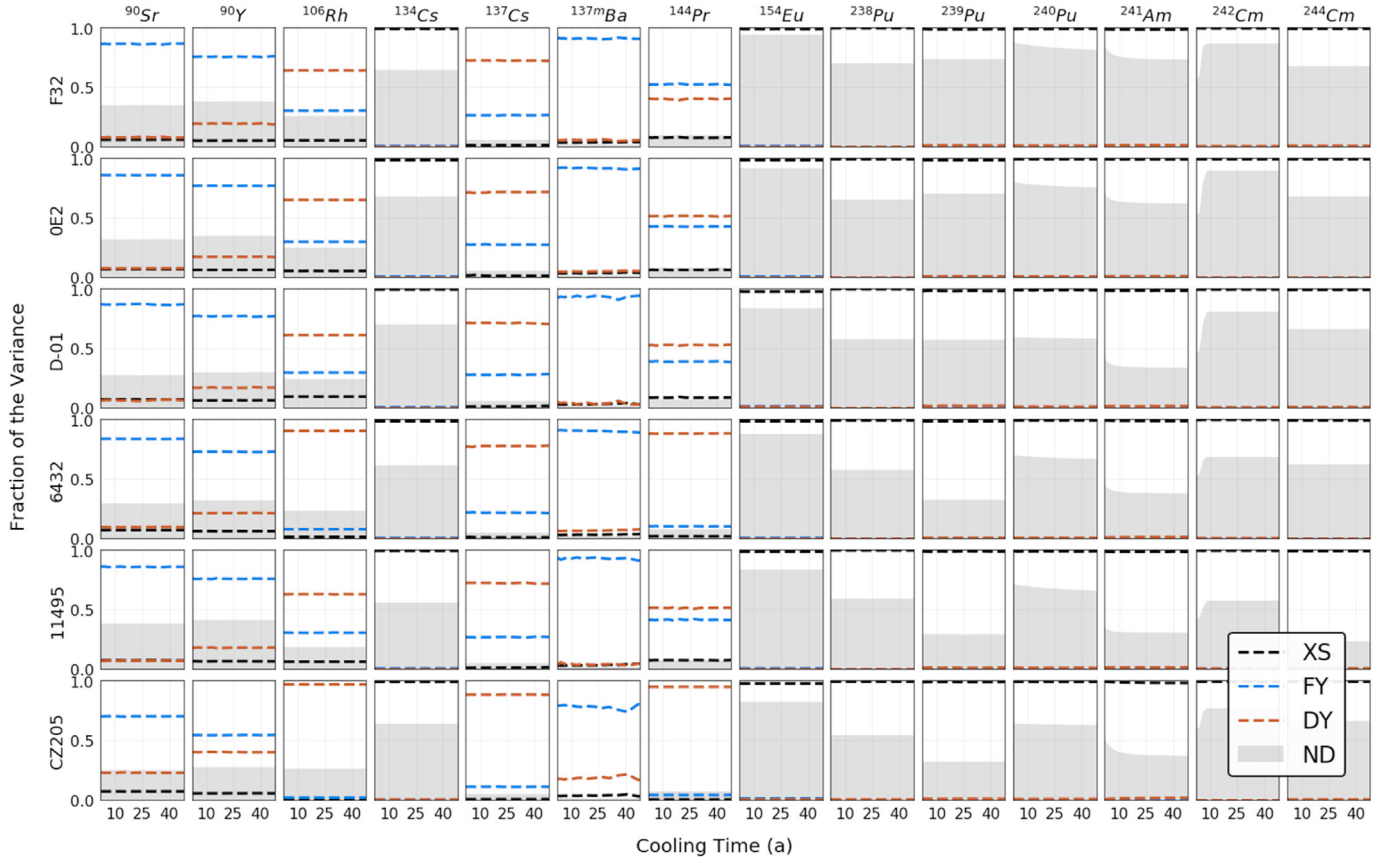

Fig. 5. Contributions of uncertainties in XS, FY, and DY to uncertainties of ND origin, and contributions of ND uncertainties to total calculational uncertainties.

106, being in transient equilibrium with their relatively longer-lived parents Ce-144 and Ru-106, also show significant contributions from FY and DY uncertainties. Cs-134 and Eu-154 show exceptionally significant contributions from XS uncertainties to their uncertainties of ND origin compared to the other F/DPs, and almost no dependence on FY and DY data. The production of the latter nuclides results mainly from irradiation and from neutron capture into Cs-133 and Eu-153 [36].

Individual implementation of the XS, FY and DY perturbations changes the corresponding nuclear data of all considered isotopes at once (in each perturbation). Perturbations of nuclide-specific nuclear data are not available in the SCALE package used. Future releases of the SCALE code system that allow these individual perturbations would also allow identification of the most relevant nuclear data reactions and uncertainties toward all decay-heat-relevant nuclide uncertainties; this is envisioned for future work.

4.6. Similarity analyses

In this section, we analyze correlations between the SFA total decay heats due to perturbations in ND and DO variables. These correlations between SFA decay heats are analyzed at the cooling times listed in Table 5, and are shown in Fig. 6, Fig. 7 and Fig. 8. Fig. 6 shows the correlations between the SFA total decay heats due to perturbations in both ND and DO variables. Similarities in burnup result in relatively higher correlations, e.g., the total decay heat in the highest burnup PWR SFA F32 is 0.96, which correlates with the highest burnup BWR SFA 6432, despite their having different DO variables and originating from a PWR and a BWR, respectively. In contrast, the decay heats for these two SFAs show fewer correlations with other low burnup SFAs of the same reactor of origin, e.g., the correlation between the highest and the lowest burnup is 0.91 for PWR SFAs and 0.87 for BWR SFAs. However, other differences between these SFAs, such as their cooling times, could change their level of correlation, as they impact nuclide-wise correlations differently, and the nuclide-wise contributions to the total decay heats are also different. In general, the SFAs analyzed in this study are highly correlated due to perturbations in both the ND and DO variables, i.e., the lowest observed correlation is 0.85.

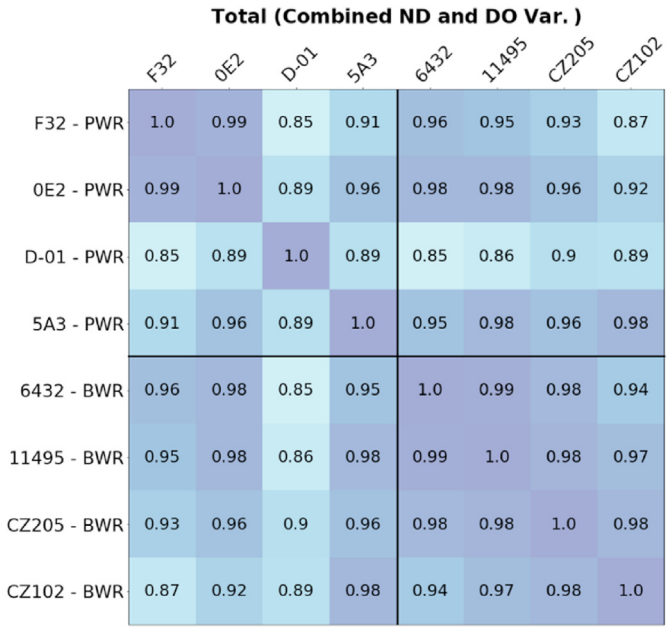

Fig. 6. Correlations between total decay heats due to perturbations of both ND and DO variables.

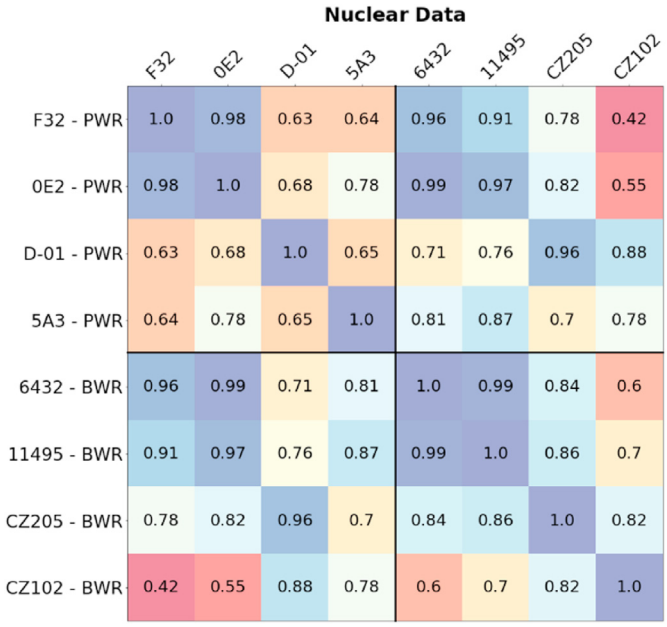

Fig. 7. Correlations between total decay heats due to perturbations of ND.

Fig. 7 shows the correlations between the SFA total decay heats due to perturbations of ND, and relatively higher correlations as a result of similarities in burnup. However, differences in burnup result in significant reductions in correlations compared to the combined perturbations of both ND and DO variables, e.g., the decay heat from the highest burnup PWR SFA F32 correlates with 0.96 to the highest burnup BWR SFA 6432, and with 0.64 to the lowest burnup PWR SFA 5A3.

Fig. 8 shows the correlations between the SFA total decay heats due to perturbations of DO variables. The SFA total decay heats tend to respond with high correlations due to perturbation in their DO variables; the BWRs showed almost unform cross-correlation, and the PWRs showed the lowest cross-correlation of 0.92. The perturbation factors of the SFA burnup, and therefore the cycle-wise powers, correlate largely and positively with the total decay heat of the SFAs. The SFA burnup is a relatively influential parameter. Enrichments, boron, and fuel density tend to show insignificant correlations to the SFA decay heat. Other DO variables that induce significant changes in neutron spectra, such as cladding radii in the PWRs and water density in the BWRs, correlate with the SFA total decay heat on various levels. Increased cladding outer dimensions (combination of the cladding thickness and its radius) or reduced water densities harden the neutron spectra, measured as spectral indices in these perturbed SFA models. Harder neutron spectra result in higher transmutation rates of U-238 and transmutation of larger fractions of decay-heat-relevant ACs. Nuclide-wise analyses show negative correlations between all of the analyzed ACs and water densities, and positive correlations between them and the cladding outer dimensions, e.g., Pu-238 and 239 correlate negatively with the water densities in all of the analyzed SFAs by less than −0.4 and −0.9, respectively. Also, these nuclides correlate with the cladding outer dimensions in all of the analyzed SFAs by more than 0.2 and 0.5, respectively. Water density has a significant impact on the BWRs compared to the PWRs, given the range of perturbations presented in Table 4. For example, in SFA F32, 1 SD of the water density is 0.7%, whereas it is 6% in SFA 6432. In the latter, we vary the void fraction, which has larger uncertainties.

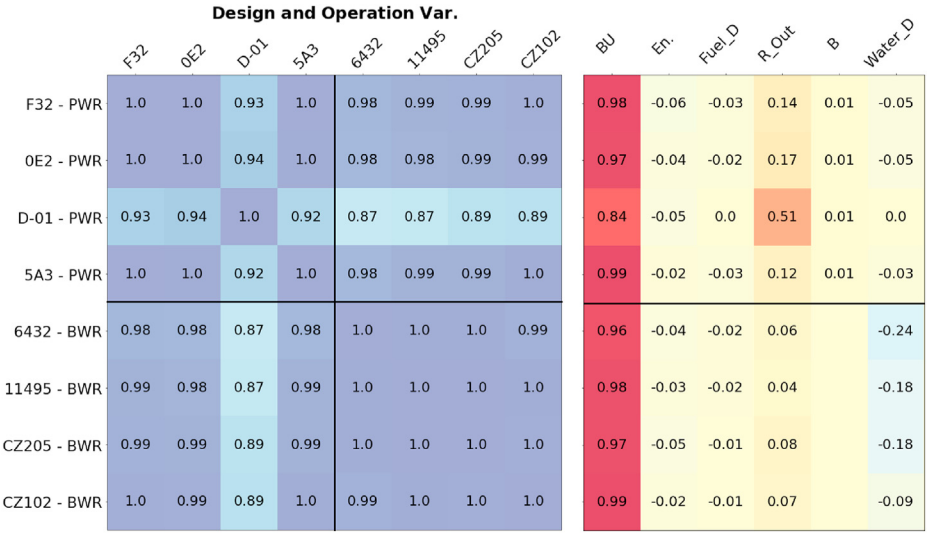

Fig. 8. Correlations between total decay heats due to perturbations of DO variables, along with correlations between total decay heats and the perturbed variables. The abbreviations in the right plot stand for: burnup, enrichment, fuel density, outer dimension of the cladding and tubing, boron in BWRs, and the water density.

4.7. Contribution of burnup uncertainties to uncertainties of DO origin

We noted that SFAs with similar burnups show large correlations in their decay heat due to ND perturbations. Also, the SFA burnup correlates significantly and positively with the total decay heat. In this section, we analyze contributions of burnup uncertainties to decay heat uncertainties focusing on SFA 6432 and using the assumptions mentioned in Section 2.2.

Case 1 with a 50% increase in the SD of all variables (including the burnup) results in an increase in the decay heat uncertainty by ~50%, between 2 and 100 years of decay, i.e., the final variances increased by almost the same percentage as the initial variances.

The other cases (Cases 2 to 6) are shown in Fig. 9. Case 2, in which all variables are uniformly distributed, shows approximately the same SD for the calculated decay heat, which is similar to the reference case in which they are normally distributed, i.e., assumptions on the form of the distributions (normal vs. uniform) are less significant.

Considering only uncertainties in the power and the fuel temperatures (Case 3) results in a gradual decrease in the decay heat uncertainties between 2 and 100 years. Uncertainties in the SFA burnup alone contribute 92% and 73% to the variances in the calculated decay heat (corresponding to 96% and 86% SDs, respectively). The decreased uncertainties mainly result from decreased uncertainties in the actinides, which are also sensitive to variables that induce spectral changes and which are excluded in this case. Case 3 shows that the burnup and its uncertainty are significant contributors to the resulting decay heat uncertainties, but to a lesser extent at longer cooling times. Accurate power history and reduction of uncertainties in the SFA burnup would result in the most significant reduction in decay heat uncertainties in the analyzed decay time.

The Cases 4 and 5 have the same burnup uncertainties, but these originate from uncertainties in the power in later irradiation cycles (Case 4), and in earlier irradiation cycles (Case 5). Uncertainties in the powers of the later irradiation cycles show increased uncertainties in the decay heat for short-term decay, and vice versa. However, and regardless of the allocation of uncertainties in cycle-wise powers along the irradiation, the longer the decay time, the more decay heat uncertainties approach the reference case. This means that different allocations of the power variances along the irradiation history are assumptions that have insignificant effect on the calculated decay heat uncertainty.

Case 6, where cycle-wise average powers are sampled independently of each other, shows a significant decrease in the

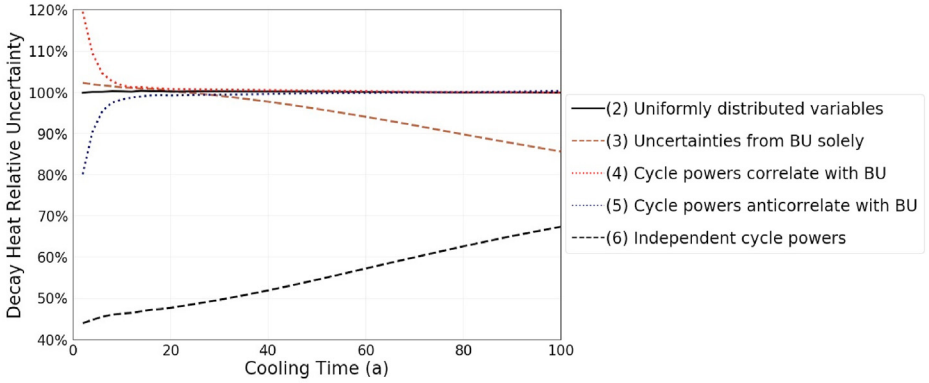

Fig. 9. Relative uncertainty (relative SD) for analyzed cases that implement different assumptions on the power and burnup distributions. The cases are relative to the reference case of SFA 6432, and their case number is shown in parentheses.

resulting decay heat uncertainties (down to 45% of the reference values). In this case, the variance of the final SFA burnup is also lower than the reference case, in which correlations between cycle-wise powers and burnup ensured the final burnup variance.

4.8. Comparison with literature studies

Previous studies on decay heat uncertainties of LWR assemblies are reported in the literature, for example for SFA 6432 by Ilas and Liljenfeldt [20], and for realistic BWR assemblies with similar burnups and cooling times by Rochman et al. [17]. Table 8 presents comparisons between the results of this work and the results in these references. The results in Ref. [20] were calculated using SCALE and the same ND libraries, using the TRITON module of SCALE. We obtained similar values for contributions from FY and XS uncertainties, which might result from using the same nuclear data and covariance information. However, we obtained larger values for contributions from uncertainties in DO variables, since the implemented DO uncertainty ranges in this work differ from those in Ref. [20].

The results in Ref. [17] were obtained using the CASMO/SIMULATE/SNF sequence, implementing fine irradiation histories and realistic boundary conditions, which may affect the propagation of input uncertainties. We obtain contributions from FY uncertainties that are almost an order of magnitude less than the results in Ref. [17]. Both this work and the reference are based on ENDF/B-VII.1 for the FY data; however, reference [17] uses developed covariance matrices for the independent yield based on information from the cumulative yields. Further analyses for processing uncertainties and correlations in FY data could resolve or pinpoint the noted discrepancies.

5. Conclusions

Design and operation (DO) and nuclear data (ND) uncertainties were propagated in simulations that calculate the decay heats from spent nuclear fuel (SNF) using SCALE/Polaris for lattice calculations and Sampler for stochastic uncertainty propagations. The models are LWR spent fuel assemblies (SFAs) that have multiple decay heat measurements and different DO variables (4 from PWRs and 4 from BWRs). Propagated uncertainties are based on SCALE-6.2 evaluations of ENDF/B-VII.1 ND and SFCOMPO-recommended ranges for DO variables. Decay heat residuals R (difference between calculations and measurements) were standardized with their uncertainties to calculate z-scores for each benchmark and combined z-scores for each SFA, with the significance level set to 0.05 in this study.

The SFAs measured at the Clab facility show that differences between their decay heat calculations and measurements are not significant. SFAs measured at GE-Morris show significantly larger z-scores and significant decay heat residuals, despite these measurements having relatively large experimental uncertainties. Random or systematic uncertainties are not accounted for in the SFAs CZ102 and CZ205 which were measured at GE-Morris and require further investigation. This also highlights the importance of the availability of high-quality decay heat measurements and operational data (similar to the SFAs measured in Clab), which results in lower biases between decay heat calculations and measurements. This also illustrates how these biases could be explained by the uncertainties of both the calculations and the measurements.

Decay heats and their uncertainties are largely attributed to 14 nuclides at average measurement times for all analyzed SFAs. The DO variables contribute more significantly to the resulting calculational uncertainties than uncertainties of ND origin. Particularly burnup, but also water densities and cladding radii, are influential variables. Burnup correlates significantly with the SFA decay heat. Also, high-burnup SFAs correlate largely with each other, and less significantly with low-burnup SFAs. The reactor of origin also shows an influence on correlations between decay heats of SFAs, albeit lower than the influence of SFA burnups. Additionally, burnup monotonically increases uncertainties of ND origin, particularly in the PWRs, as well as the buildup of decay heat relevant nuclides. Such observations pinpoint that providing a proper account of burnup and its uncertainty could improve calculations and resolve a large component of decay-heat-related calculational uncertainties. The standard deviation of the burnup and the correlations between the cycle-wise powers are significant assumptions. How this distribution is shaped and whether uncertainties originate from earlier or later cycles, are less significant assumptions. Also, observations of high correlations between decay heats from nuclides and assembly-wise values, particularly between high-burnup SFAs, could be supported by future sensitivity analyses.

The influencing ND with regard to uncertainties of the decay heats from actinides are cross-sections, whereas they are varying contributions from cross-sections, fission yields, and decay data for the fission and decay products. Additionally, availability of high-quality ND would reduce their relatively large contribution to decay heat uncertainties, particularly in the high-burnup SFAs. The highest burnup in the present study is 51 GWd/tU, which is a moderate value with respect to recent typical discharge burnups. Analysis of ND contributions at higher burnups is suggested for future work.

The uncertainties obtained are relatively high with respect to applications that rely on calculations, such as loading optimization of disposal canisters. For instance, the total calculated uncertainty is 5.6% for an SFA that has 51 GWd/tU. Such value can potentially increase the total number of canisters required to comply with the maximum permissible 1500 W limit per canister, particularly when shorter cooling times apply to canister loading. At high burnup, DO variables contribute significantly to these uncertainties, and the increased accuracy of DO variables such as accurate burnup values would reduce both the resulting uncertainties of DO origin and the overall uncertainties.

An assessment of nuclide-specific fission yields and cross-sections impacting the uncertainties of such nuclides could not be analyzed in the current study due to limitations of the SCALE version used (6.2), which is envisioned in future work using SCALE

Table 8
Comparison with uncertainty values reported in Refs. [17,20]. All uncertainties in this table are expressed as 1σ.

Cooling (a)	Burnup (GWd/tU)	U-235 wt%	SFA ID	Uncertainty %				Ref.
				FY	XS	ND	DO	
15	37.3	3.0	Assembly-1	2.31	–	2.30	–	[17]
15	36.8	3.0	Assembly-2	2.20	–	2.30	–	[17]
15.6	36.9	2.9	6432	0.26	0.88	–	0.87	[20]
15.6	36.9	2.9	6432	0.24	0.89	0.91	2.11	This work

releases that would have these capabilities. Analyses of fission yield uncertainties are required to assess inconsistencies between the results of this work and reference results in the literature. Additionally, this work aimed at selecting SFAs that are different from each other with respect to their DO variables. Nevertheless, analyses of the correlation of their decay heat show that the analyzed SFAs have significant similarities with respect to their decay heat responses to perturbations in ND and DO variables. Further analyses could be performed in the future for decay heat benchmarks with larger differences in their DO variables, e.g., higher enrichments, burnups, and also MOX-based SFAs.

Declaration of competing interest

The authors declare that they have no known competing financial interests or personal relationships that could have appeared to influence the work reported in this paper.

Acknowledgments

This study is part of an ongoing PhD project titled “Uncertainty quantification of spent nuclear fuel nuclide inventory” that is funded by the Swiss National Cooperative for the Disposal of Radioactive Waste (Nagra). This study was also partly funded by the European Union's Horizon 2020 Research and Innovation Programme under Grant Agreement No. 847593.

References

[1] A. Shama, D. Rochman, S. Caruso, A. Pautz, Validation of spent nuclear fuel decay heat calculations using Polaris, TRITON/ORIGEN-ARP, and CASMO5, Ann. Nucl. Energy (2021). Submitted for publication.
[2] Nagra, The Nagra Research, Development and Demonstration (RD&D) Plan for the Disposal of Radioactive Waste in Switzerland, 2016. Technical Report 16-02, Switzerland, https://www.nagra.ch/display.cfm/id/102495/disp_type/display/filename/e_ntb16-02.pdf.
[3] ENSI, Specific Design Principles for Deep Geological Repositories and Requirements for the Safety Case, Guideline ENSI-G03, ENSI, Switzerland, 2009. www.ensi.ch/en/wp-content/uploads/sites/5/2011/08/g-003_e.pdf.
[4] & SKB. Posiva, Safety Functions, Performance Targets and Technical Design Requirements for a KBS-3V Repository - Conclusions and Recommendations from a Joint SKB and Posiva Working Group, Posiva SKB Report 01, ISSN 2489-2742, Posiva, Finland; SKB, Sweden, 2017. https://www.skb.se/publikation/2485568/Posiva+SKB+Report+01.pdf.
[5] I.C. Gauld, G. Illas, B.D. Murphy, C.F. Weber, Validation of SCALE 5 Decay Heat Predictions for LWR Spent Nuclear Fuel, NUREG/CR-6972, ORNL/TM-2008/015, ORNL (Oak Ridge National Laboratory), Oak Ridge, Tennesse, USA, 2010.
[6] G. Ilas, I.C. Gauld, H. Liljenfeldt, Validation of ORIGEN for LWR used fuel decay heat analysis with SCALE, Nucl. Eng. Des. 273 (2014) 58–67, https://doi.org/10.1016/j.nucengdes.2014.02.026.
[7] G. Ilas, I.C. Gauld, SCALE analysis of CLAB decay heat measurements for LWR spent fuel assemblies, Ann. Nucl. Energy 35 (2008) 37–48, https://doi.org/10.1016/j.anucene.2007.05.017.
[8] J.-C. Sublet, JEFF-3.1, ENDF/B-VII and JENDL-3.3 critical assemblies benchmarking with the Monte Carlo code TRIPOLI, IEEE Trans. Nucl. Sci. 55 (2008) 604–613, https://doi.org/10.1109/TNS.2007.911600.
[9] L. San Felice, R. Eschbach, R. Dewi Syarifah, S.-E. Maryam, K. Hesketh, MOx Depletion Calculation Benchmark, Organisation for Economic Co-Operation and Development, 2016. http://inis.iaea.org/Search/search.aspx?orig_q=RN:49042360. (Accessed 20 August 2020).
[10] B. Roque, R. Gregg, R. Kilger, F. Laugier, P. Marimbeau, A. Ranta-Aho, C. Riffard, K. Suyama, J.F. Thro, M. Yudkevich, K. Hesketh, E. Sartori, International comparison of a depletion calculation benchmark devoted to fuel cycle issues results from the phase 1 dedicated to PWR-UOx fuels. http://inis.iaea.org/Search/search.aspx?orig_q=RN:43130067, 2006. (Accessed 19 August 2020).
[11] Burn-up credit criticality benchmark: phase IV-A: reactivity prediction calculations for infinite arrays of PWR MOX fuel pin cells, (n.d.). https://www.oecd-ilibrary.org/nuclear-energy/burn-up-credit-criticality-benchmark_9789264103498-en. (Accessed 19 August 2020).
[12] I. Gauld, U. Mertyurek, Margins for Uncertainty in the Predicted Spent Fuel Isotopic Inventories for BWR Burnup Credit, NUREG/CR-7251, U.S. NRC, ORNL (Oak Ridge National Laboratory), 2018.
[13] G. Radulescu, I.C. Gauld, G. Ilas, J.C. Wagner, Approach for validating actinide and fission product compositions for burnup credit criticality safety analyses, Nucl. Technol. 188 (2014) 154–171, https://doi.org/10.13182/NT13-154.
[14] B.T. Bearden, M.A. Jessee, SCALE Code System, ORNL/TM-2005/39, Oak Ridge National Laboratory, Oak Ridge, Tennessee, USA, 2018.
[15] SKB, Measurements of Decay Heat in Spent Nuclear Fuel at the Swedish Interim Storage Facility, Clab, R-05-62, Svensk Kärnbränslehantering AB (SKB), Sweden, 2006. https://www.skb.se/publikation/1472024/R-05-62.pdf.
[16] M.A. McKinnon, C.M. Heeb, J.M. Creer, Decay Heat Measurements and Predictions of BWR Spent Fuel, EPRI NP-4619, Electric Power Research Institute, EPRI, 1986.
[17] D.A. Rochman, A. Vasiliev, A. Dokhane, H. Ferroukhi, Uncertainties for Swiss LWR spent nuclear fuels due to nuclear data, EPJ Nucl. Sci. Technol. 4 (2018) 6, https://doi.org/10.1051/epjn/2018005.
[18] N. García-Herranz, O. Cabellos, F. Álvarez-Velarde, J. Sanz, E.M. González-Romero, J. Juan, Nuclear data requirements for the ADS conceptual design EFIT: uncertainty and sensitivity study, Ann. Nucl. Energy 37 (2010) 1570–1579, https://doi.org/10.1016/j.anucene.2010.06.006.
[19] D. Rochman, A. Vasiliev, H. Ferroukhi, T. Zhu, S.C. van der Marck, A.J. Koning, Nuclear data uncertainty for criticality-safety: Monte Carlo vs. linear perturbation, Ann. Nucl. Energy 92 (2016) 150–160, https://doi.org/10.1016/j.anucene.2016.01.042.
[20] G. Ilas, H. Liljenfeldt, Decay heat uncertainty for BWR used fuel due to modeling and nuclear data uncertainties, Nucl. Eng. Des. 319 (2017) 176–184, https://doi.org/10.1016/j.nucengdes.2017.05.009.
[21] O. Leray, D. Rochman, P. Grimm, H. Ferroukhi, A. Vasiliev, M. Hursin, G. Perret, A. Pautz, Nuclear data uncertainty propagation on spent fuel nuclide compositions, Ann. Nucl. Energy 94 (2016) 603–611, https://doi.org/10.1016/j.anucene.2016.03.023.
[22] M.L. Williams, G. Ilas, M.A. Jessee, B.T. Bearden, D. Wiarda, L. Zwermann, M. Gallner, M. Klein, B. Krzykacz–Hausmann, A. Pautz, A statistical sampling method for uncertainty analysis with SCALE and XSUSA, Nucl. Technol. 183 (2013) 515–526.
[23] W. Wieselquist, T. Zhu, A. Vasiliev, H. Ferroukhi, PSI methodologies for nuclear data uncertainty propagation with CASMO-5M and MCNPX: results for OECD/NEA UAM benchmark phase I, Sci. Technol. Nucl. Install. (2013), e549793, https://doi.org/10.1155/2013/549793, 2013.
[24] Nuclear Science Committee, Working Party on Nuclear Criticality Safety (WPNCS), Expert Group on Assay Data of Spent Nuclear Fuel (EGADSNF), Evaluation Guide for the Evaluated Spent Nuclear Fuel Assay Database (SFCOMPO), NEA/NSC/R, vol. 8, OCED/NEA, 2016. https://www.oecd-nea.org/science/docs/2015/nsc-r2015-8.pdf.
[25] European Joint Programme on Radioactive Waste Management (EURAD), EU H2020-Euratom-1.2 program, 2020. https://cordis.europa.eu/project/id/847593 (accessed December 28, 2020).
[26] P. Jansson, M. Bengtsson, U. Bäckström, K. Svensson, M. Lycksell, A. Sjöland, Data from calorimetric decay heat measurements of five used PWR 17x17 nuclear fuel assemblies, Data Brief 28 (2020) 104917, https://doi.org/10.1016/j.dib.2019.104917.
[27] L.E. Wiles, N.J. Lornbardo, C.M. Heeh, U.P. Jenquin, T.E. Michener, C.L. Wheeler, J.M. Creer, R.A. McCann, BWR Spent Fuel Storage Cask Performance. Pre-and Post-Test Decay Heat, Heat Transfer, and Shielding Analyses, PNL-5777 Vol. II, USA, 1986.
[28] M.A. McKinnon, J.W. Doman, J.E. Tanner, R.J. Guenther, J.M. Creer, C.E. King, BWR Spent Fuel Storage Cask Performance. Cask Handling Experience and Decay Heat, Heat Transfer, and Shielding Data, PNL-5777, vol. I, 1986. USA.
[29] F. Michel-Sendis, I. Gauld, J.S. Martinez, C. Alejano, M. Bossant, D. Boulanger, O. Cabellos, V. Chrapciak, J. Conde, I. Fast, M. Gren, K. Govers, M. Gysemans, V. Hannstein, F. Havlůj, M. Hennebach, G. Hordosy, G. Ilas, R. Kilger, R. Mills, D. Mountford, P. Ortego, G. Radulescu, M. Rahimi, A. Ranta-Aho, K. Rantamäki, B. Ruprecht, N. Soppera, M. Stuke, K. Suyama, S. Tittelbach, C. Tore, S.V. Winckel, A. Vasiliev, T. Watanabe, T. Yamamoto, T. Yamamoto, SFCOMPO-2.0: an OECD NEA database of spent nuclear fuel isotopic assays, reactor design specifications, and operating data, Ann. Nucl. Energy 110 (2017) 779–788, https://doi.org/10.1016/j.anucene.2017.07.022.
[30] P.J. Turinsky, Core isotopic depletion and fuel management, in: D.G. Cacuci (Ed.), Handb. Nucl. Eng., Springer US, Boston, MA, 2010, pp. 1241–1312, https://doi.org/10.1007/978-0-387-98149-9_10.
[31] H.T. Hayslett, P. Murphy, Statistics, Elsevier, 1981, https://doi.org/10.1016/C2013-0-01181-4.
[32] N.R. Draper, in: fourth ed., in: B.S. Everitt, A. Skrondal (Eds.), The Cambridge Dictionary of Statistics, vol. 79, 2011, pp. 273–274, https://doi.org/10.1111/j.1751-5823.2011.00149_2.x. Int. Stat. Rev.
[33] S.A. Stouffer, E.A. Suchman, L.C. Devinney, S.A. Star, R.M. Williams, The American Soldier: Adjustment during Army Life. Studies in Social Psychology in World War II, Princeton University Press, Princeton, NJ, 1949.
[34] J.D. Evans, Straightforward Statistics for the Behavioral Sciences, Brooks/Cole Pub. Co., Pacific Grove, 1996.
[35] N. Soppera, M. Bossant, E. Dupont, JANIS 4: an improved version of the NEA java-based nuclear data information system, Nucl. Data Sheets 120 (2014) 294–296, https://doi.org/10.1016/j.nds.2014.07.071.
[36] H. Ezure, Calculation of atom ratios of 134Cs/137Cs, 154Eu/137Cs and Pu/U, burnup and most probable production amount of plutonium in fuel assemblies of JPDR-1, J. Nucl. Sci. Technol. 27 (1990) 562–571, https://doi.org/10.1080/18811248.1990.9731221.